Second Harmonic Generation Microscope
Design Description Document

Harmonigenic/ Dr. Robert Hill

Faculty Advisor: Dr. Wayne Knox

James Emery (Scribe)
Ava Hurlock (Document Handler)
Jordan Rabinowitz (Project Coordinator)
Yuanchao Wang (Customer Liaison)

Document Number 0002

Revisions Level	Date
Final	05-06-2018

Revision History

Rev	Description	Date	Authorization
1	Initial Document	01-22-2018	All
2	Second DDD	02-05-2018	All
3	Third DDD	02-19-2018	All
4	Midterm DDD	02-26-2018	All
5	Fourth DDD	04-02-2018	All
6	Final DDD	05-06-2018	All

Table of Contents

Vision:

The product is a prototype system for scanning and predicting metastasis in breast cancer cells. Our deliverable is a series of recommendations for how the current lab setup can be improved for a company prototype.

Project Scope:

We intend to optimize a scanning system in order to make accurate and repeatable measurements of F/B to objectively predict tumor metastasis. We are responsible for improving the signal to noise threefold, optimizing signal strength, and not damaging the sample by oversaturation. The signal strength will be optimized for the following parameters: laser wavelength within the tuning range of the Ti-Saph Laser (700 - 1000 nm), laser average pulse power, laser repetition/pulse rate, dwell time of the optical scanner, choice of numerical aperture for focusing and collection optics, and polarization of incident light and analyzer orientation. The stipulations for not damaging the sample include: the SHG signal cannot change the collagen structure (detectable as a decrease in SHG signal intensity), Paraffin (used for sample fixing) cannot melt, and we must avoid creating autofluorescent or two-photon fluorescent signals, or at least understand and know how to remove this signal. The system uses a pulsed titanium-sapphire laser to illuminate the sample, two microscope objectives (forward, backward) one to focus the beam into the sample and both to be used as collection optics, and a detector that is optimized for SHG signal wavelength.

Project Timeline:

January 16: Meeting with Dr Hill to discuss Photonics West Startup Challenge pitch.

January 19: Brief meeting with Dr Knox to plan lab tour.

January 22: Knox lab tour.

January 24: Meeting with Dr Hill to plan Brown lab research track.

February 5: Training for Knox lab

February 7: Training for Brown lab

February 9: Preliminary Research in Brown Lab

March 2: Meeting with Dr. Hill

March 7: Meeting with Dr. Brown to discuss testing

March 28: Testing in Brown Lab

April 2: Meeting with Dr. Knox

April 5: Testing in Knox Lab

April 6: Testing in Brown Lab

April 13: Meeting with Dr. Hill and Dr. Brown

April 19: Testing in Brown Lab

April 20: Final Design Review

May 4: Design Day

Starting Point:

In Dr Brown's lab, we started with the current SHG microscopy setup without any modifications to components. We started at the standard input power already used for collagen imaging, and incremented the power until the output significantly deviates from the expected SHG signal (see figure 1).

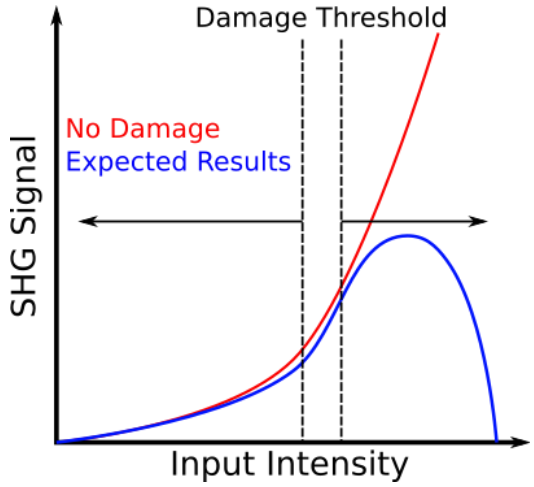

Figure 1. The expected change in SHG signal strength as a function of input laser power assuming no sample damage (red), and expected results on real samples (blue).

The study will conclude when it is confidently known what the highest input power can be that does not damage the biopsy samples.

System Setup:

Sample Preparation:

We were provided with breast tissue biopsy samples prepared with either H&E staining and paraffin fixing. They are arranged in tissue microarrays (TMAs) of 5μm thick samples. Both sample types were be measured to test susceptibility to melting, sample damage, or generation of fluorescent signals.

Findings from Preliminary Research:

Data stacks of 8 frames were taken on a single element of a tissue microarray (TMA) provided by Dr Hill. The laser power was started at the minimum that could be detected by the PMT's, and increased by 20 mW for each successive image stack. This process continued until the forward PMT, which receives more light than the backward PMT, was showing saturation on more than roughly one third of its scan area. At this point, the maximum power for the forward PMT was recorded, and the forward PMT was turned off. The process continued for just the backward PMT until it too was saturated. Results for the maximum power before saturation are shown below.

PMT Channel	Input Power	Calculated Power in Focal Volume	Visual Signs of Sample Damage	Observation of I^2 Drop-off
Forward	150 mW	24 mW	No	No
Backward	310 mW	50 mW	No	No

Table 1. The maximum input powers that give recordable signals to the PMTs in the current microscope setup. Measured input is read up the beam path, before travelling through the microscope. Actual input is estimated to be 16% of the measured input power, as provided by the lab research group.

Afterwards, the TMA element that was imaged was visually inspected for any obvious signs of damage, which could include burnt spots or bubbles. No obvious damage was observed.

The SHG intensity from the forward and backward detectors are plotted below in figure 2. We expect some falloff in the higher regimes due to detector saturation which yields uncounted signal. Both the forward and backward detectors show a quadratic increase with respect to input power before they reached their saturation limits. This behavior was expected from the I^2 model of SHG light, therefore, these plots do not suggest that the laser has fundamentally changed or damaged the sample.

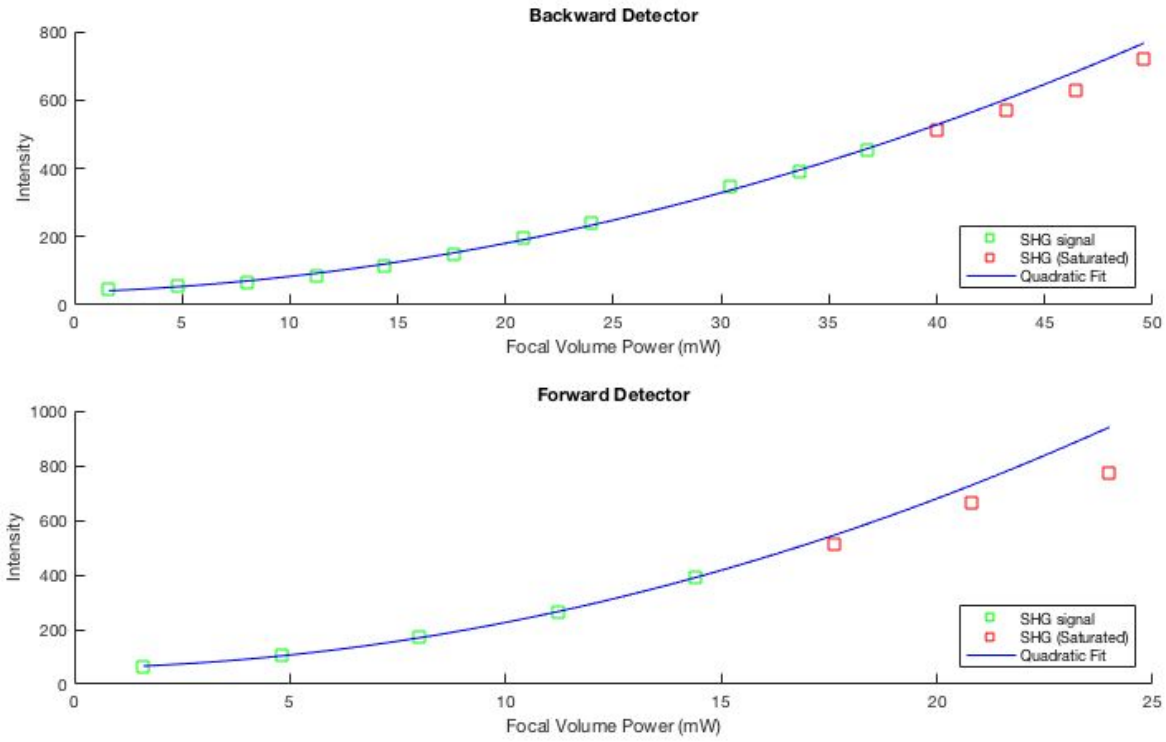

Figure 2. Plot of SHG signal as a function of input power. As power is increased we expect the intensity to increase quadratically. Each data point represents an image taken on the same location of a single sample of breast tissue in a TMA and is normalized by calculating the average pixel value (dividing total pixel counts by 1024^2) Highly saturated images (Shown in red) are excluded from the polynomial fit because they are not representative of the total signal.

Figure 2 indicates that tissue samples tend to be more strongly forward scattering, allowing the forward detector to be less sensitive than the backward detector. Therefore, one of our recommendations is to use a lower quality, less sensitive detector to reduce unnecessary costs.

Forward to Backward Ratio vs Power

The metric used by Harmonegenic to predict metastasis is the ratio of the forward to backward scattered light (F/B ratio). Therefore, it is important to track this metric and ensure that increasing the incident light is not changing the F/B ratio.

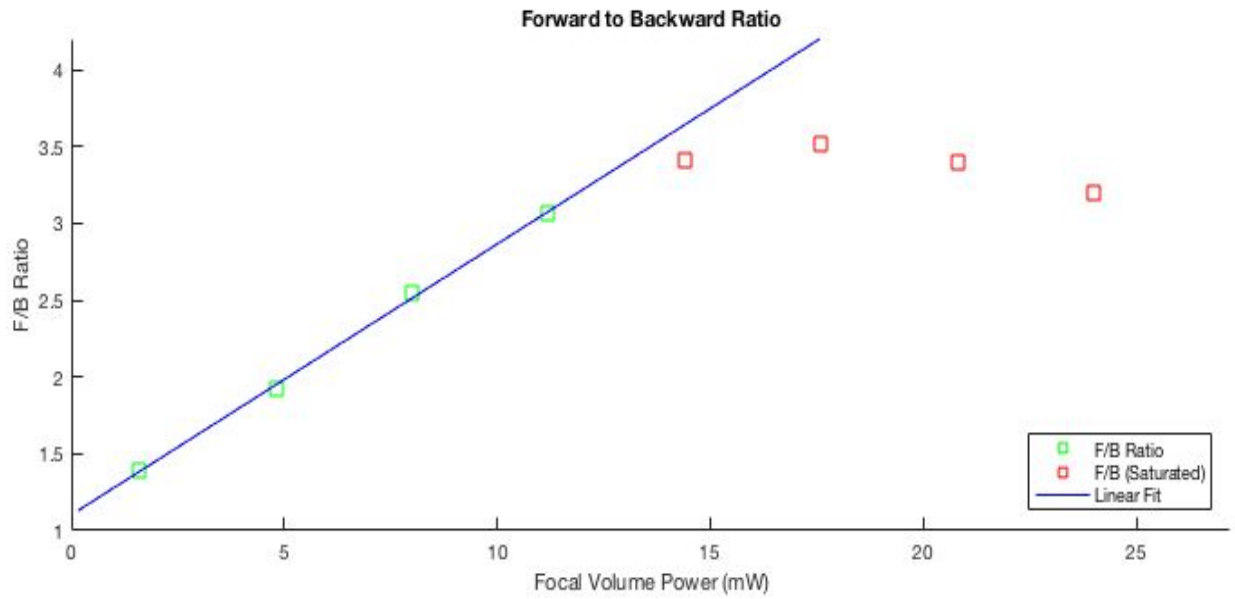

Figure 3. Forward to backward ratio as a function of power. The linear increase at low powers was not expected based on the model of SHG light. Saturated images (shown in red) are excluded from the first order polynomial fit. A possible explanation is the proximity to the noise floor, the team plans to use a more robust dark noise processing routine in future tests.

These results are complicated. The inflection point at ~15 mW is likely caused by the saturation of the forward detector thereby decreasing the forward signal. However, the linear increase in F/B in the low power region is not expected. This suggests that the signal in the forward detector is growing at a rate greater than the backward signal as the laser power is increased. This suggests that something about the sample may be fundamentally changing which causes it to emit more in the forward direction then the back at higher powers. This is an unexpected result that requires further investigation. A possible explanation for this result is the backward's detector's high noise level due to proximity to the PMT noise floor at very low powers (See Experiment 1 data tables). While it is possible that there is an error in our experimental design, we would like a future senior design group to extend our dosimetry experiment and confirm this unexpected result at higher powers.

Dosimetry Results:

In later visits, we measured SHG in the backward channel only. One of the goals was to get data at much higher input powers to observe whether signal to noise could be improved by using higher laser powers and attenuating the beam so as to not saturate the detector. As described in the results above, the higher laser powers were attenuated by placing stacks of lens paper directly in front of the PMT.

Dark Noise Correction and Laser Leakage:

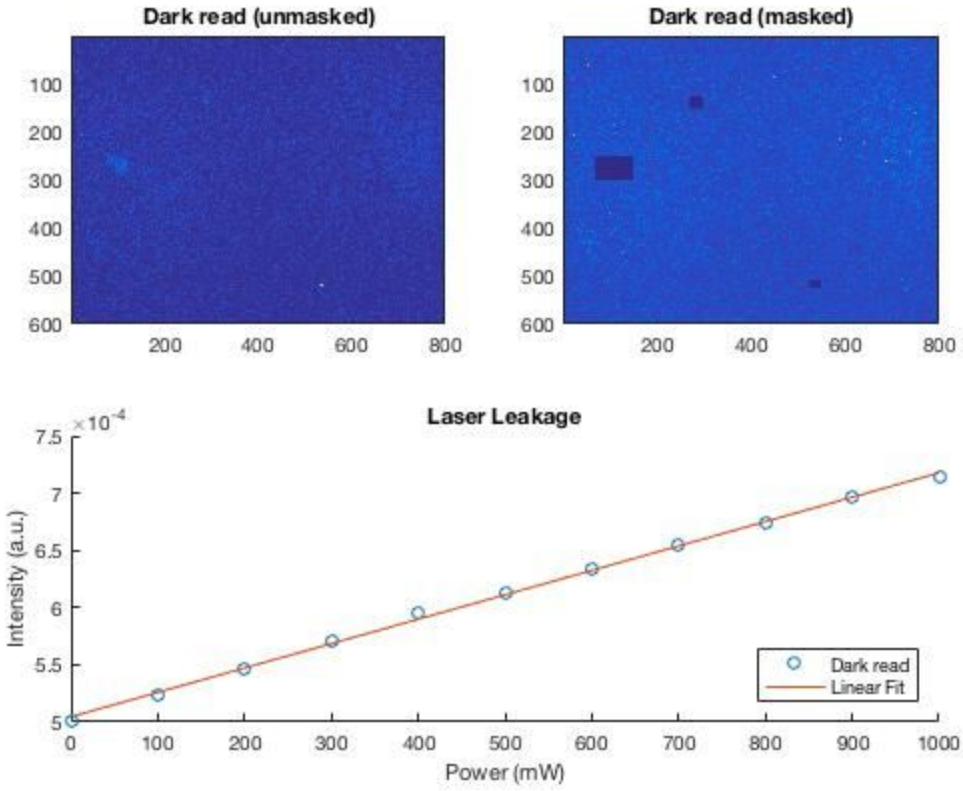

Figure 6. False-color images of the detector dark reads with (top-left) and without (top-right) a mask, which was added to eliminate bright areas of noise. The bottom graph shows the average laser leakage intensity (expected to be the only source of light on the detectors) as a function of input power.

Laser leakage was calculated by preparing an empty sample chamber and steadily increasing the input power. A lower linear relationship was found between photocurrent and input power. This implies some laser power is leaking past the excitation filters and is collected by the PMT. This can be significant at high power, so a function was developed to more correctly eliminate this leaked signal.

Dosimetry Results (Backward Detector)

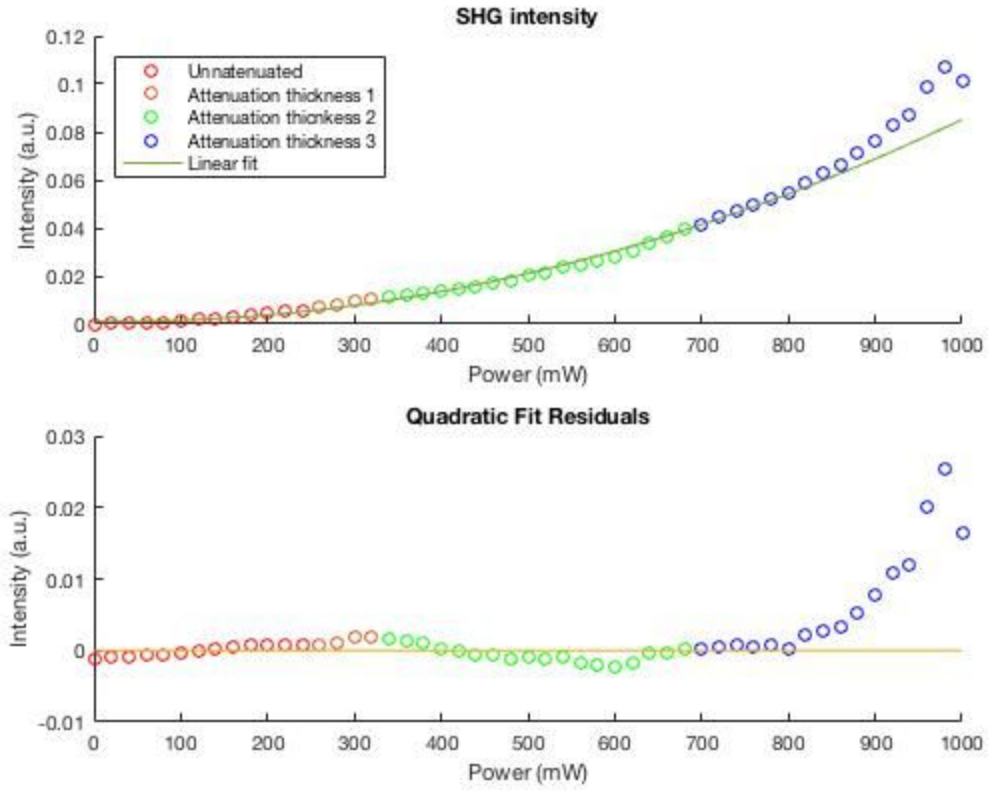

Figure 7. Average image intensity as a function of input laser power (top), along with a linear fit. Below we show the residuals from a quadratic fit to the top graph. Red circles indicate un-attenuated light, orange circles indicate light attenuated with 8 layers of lens paper, green indicates 16 layers, and blue indicates 24 layers.

The dosimetry data was prepared with a TMA in the sample chamber. Input power was linearly increased at 20 mW intervals starting at 0mW and increased to 1W. The mean pixel count was recorded at each of these powers and is plotted above. The change in color indicates a change in the signal attenuation procedure.

These data follow a quadratic fit with good precision until very high powers are achieved. This breaks off at high powers where the signal deviated above the quadratic fit. It is expected that the increase in power is due to other sources of signal, such as auto-fluorescence or fluorescence contributing to the measurements. It was decided that an initial upper limit of 800 mW should be used to avoid this unexpected behavior.

Sample Damage Indicators:

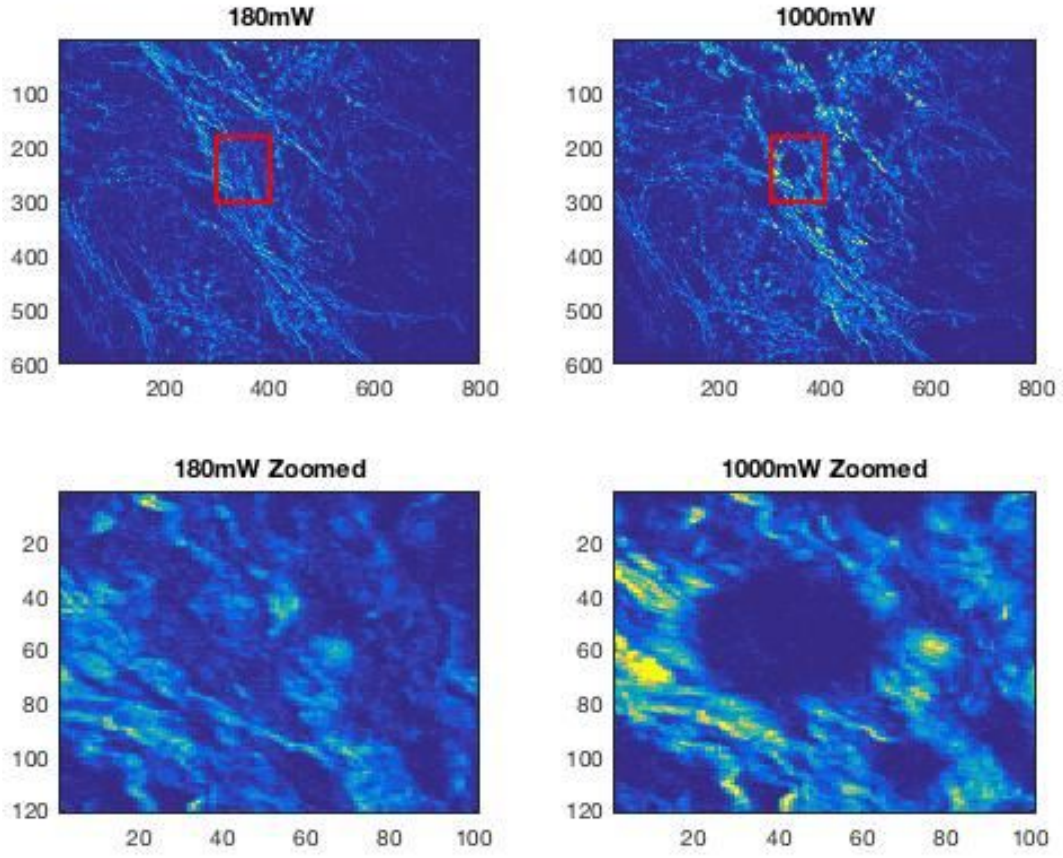

Figure 8. Some false-colored examples of sample damage as power is increased from 180 mW (top-left) to 1000 mW (top-right). The red boxes indicate a zoomed view, shown below the respective original image. These images served as the basis for indications of sample damage, as they showed bubbles of no SHG signal appearing after laser power was increased.

Sample damage was observed at high powers. This damage is visible in the effects in the sample. These bubbles show areas of signal drop off, caused by frying the collagen.

Sample damage can also be observed as a drop-off in SHG signal intensity from the expected I^2 behavior predicted in figure 1. In figure 9, below, we show that laser power significantly drops off past approximately 600 mW of input power.

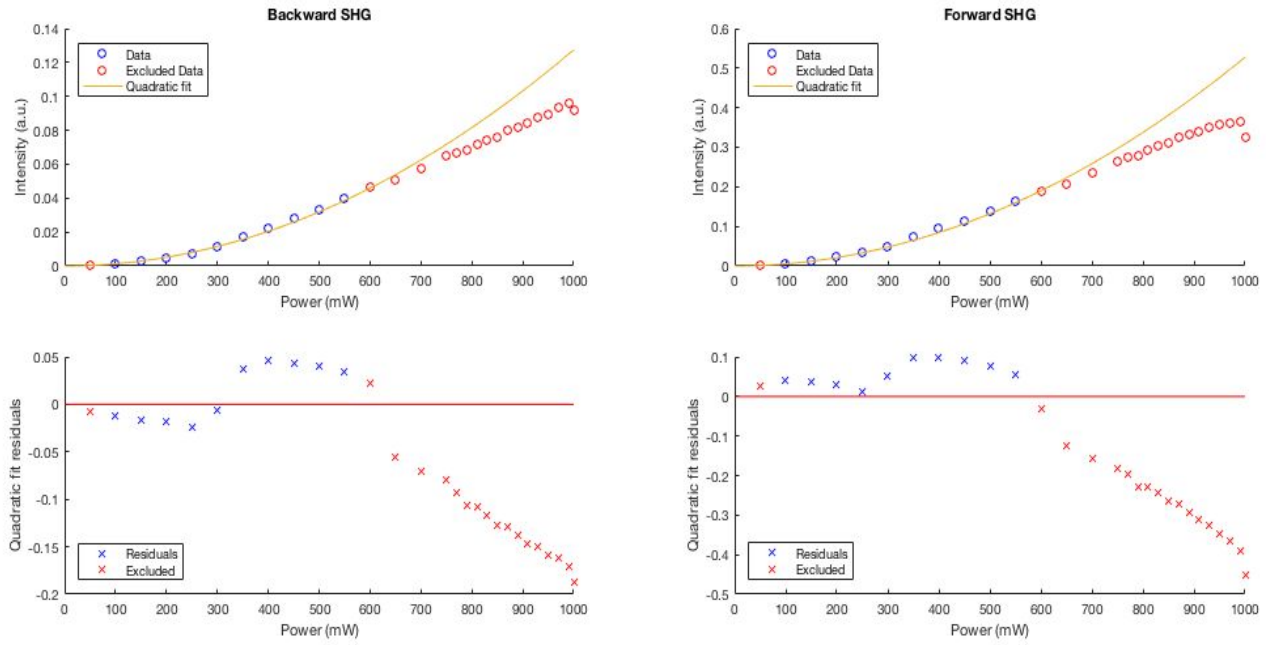

Figure 9. We show backward (top-left) and forward (top-right) SHG signal as a function of input laser power.

Our findings shown in figure 9 indicate that samples can be changed even without visible signs of damage, and prompted us to update our recommended power level to 600 mW in order to prevent this drop in SHG signal.

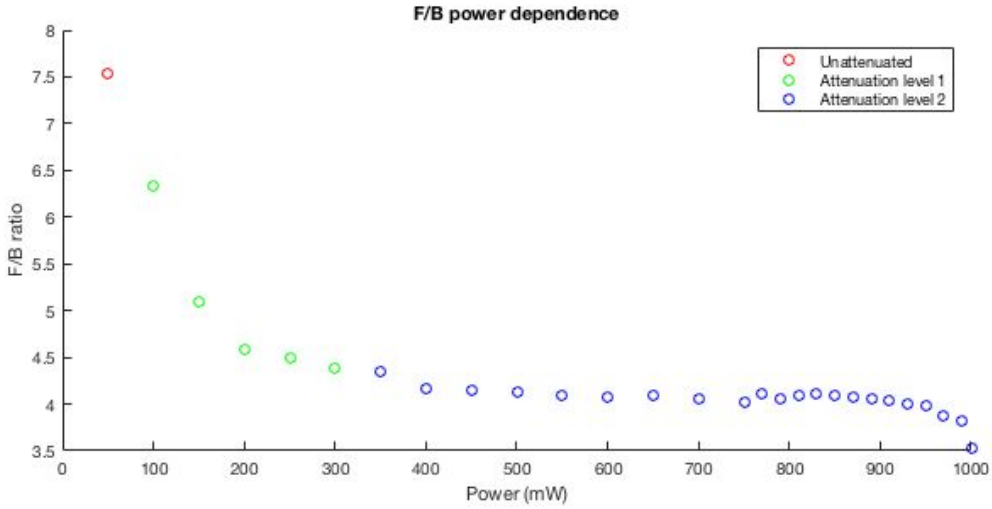

Figure 10. The dependence of F/B on input laser power. Red circles indicate no laser attenuation, green circles indicate attenuation using 8 layers of lens paper on both detectors, and blue circles indicate attenuation using 16 sheets of lens paper. The data shown was adjusted for attenuation in the image processing routine.

Sample Damage over Time:

To measure how long it takes for a sample to become visibly damaged, different areas of the TMA were exposed to constant powers and scanned at constant intervals after the power was first turned on. These experiments were expected to give an idea of how long samples can be kept under increased power inputs before they incur damage. Separate elements of the TMA were imaged at 500, 600, 700, and 800 mW over time until they showed significant damage. In this case, a sample was considered "damaged when there were visible dark, circular areas on the image that were not part of the original image. From each image, normalized intensities were calculated by averaging over a constant area. Figure 10 displays these images and our results are shown below in figure 11.

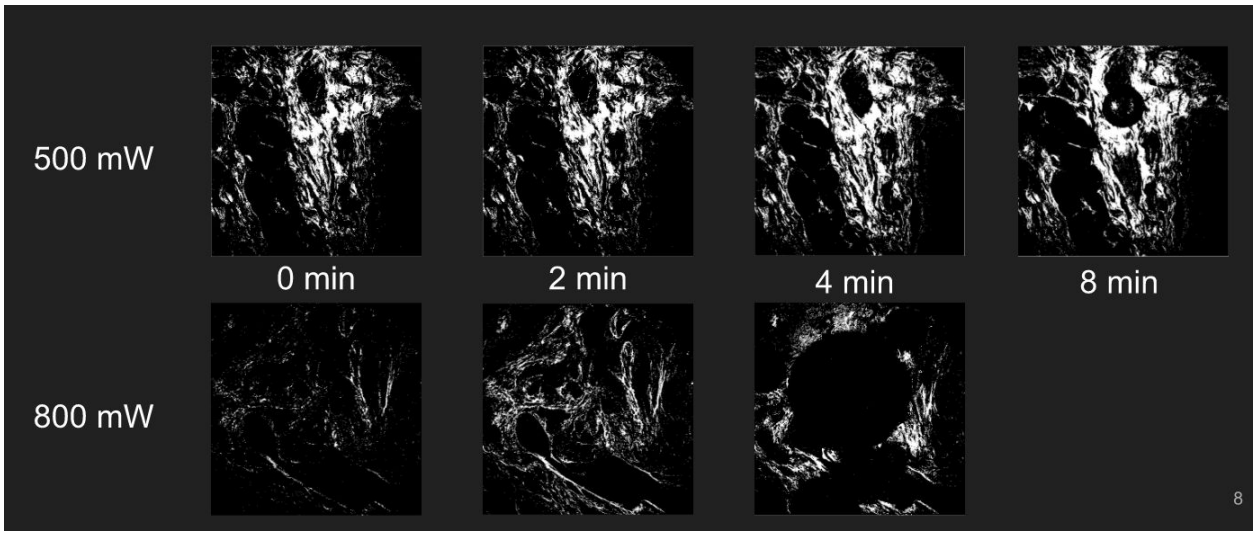

Figure 10: Sample damage at 500 mW and 800 mW over time. These images are the result of tests measuring how high the power could be increased and for how long. At 500mW, the sample remained intact for ~6 minutes whereas at 800mW the sample was burned within 2 minutes. We used these results to plot the figure below.

To quantitatively determine the signal drop-off as samples became damaged, we also calculated the average normalized intensity of the SHG signal of the four power levels as a function of time, shown below in figure 11.

Given the evidence that tissue slices can be kept intact under the microscope for a few minutes, we recommend that a commercial version of this scanner use a simpler x-y translation stage to scan samples rather than the unnecessarily fast and expensive galvanometer system currently used.

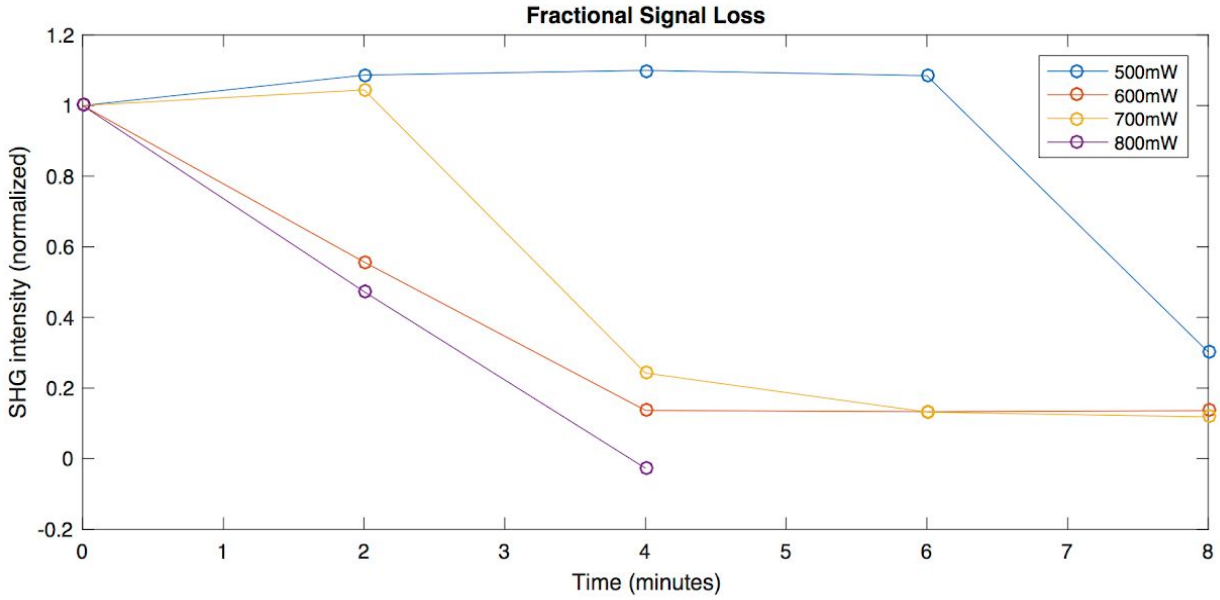

Figure 11. Normalized SHG intensities of different elements at different powers (500-800 mW) over time. Our findings indicate that a sample is unlikely to withstand significant scanning times at 700 or 800 mW. It appears most beneficial for a sample to be scanned at 5-6 min at 500 mW.

Based on these results, we suggest updating the recommended scanning power to 500 mW because it gives significantly more signal than the previously-used 100 mW, and allows the sample to be scanned for much longer than slightly higher powers such as 600 mW.

HDR Image Processing Results:

As suggested by our advisor Dr Knox, we used the High Dynamic Range (HDR) toolbox for MATLAB to overcome the dynamic range limitations of the Brown lab setup.[1] Since exposure time was not varied in the first set of experiments, we treated the square of relative input power as an equivalent parameter, following the relation of input power to SHG signal, shown below in equation 1:

$$I_{SHG} \propto I_{In}^{2} \quad (1)$$

where I_{SHG} is the intensity of the output SHG and I_{un} is the input intensity from the laser. If we assume that the sample and detector response are linear, then inputting the square of the relative intensities will be equivalent to exposure times.

The following plots suggest the benefit of using HDR processing for our data set. At low powers (top plot) we can best resolve high signal regions without saturating the detectors and we can used overexposed saturated images (bottom plot) to increase contrast on low signal regions like the area on the left of the plot.

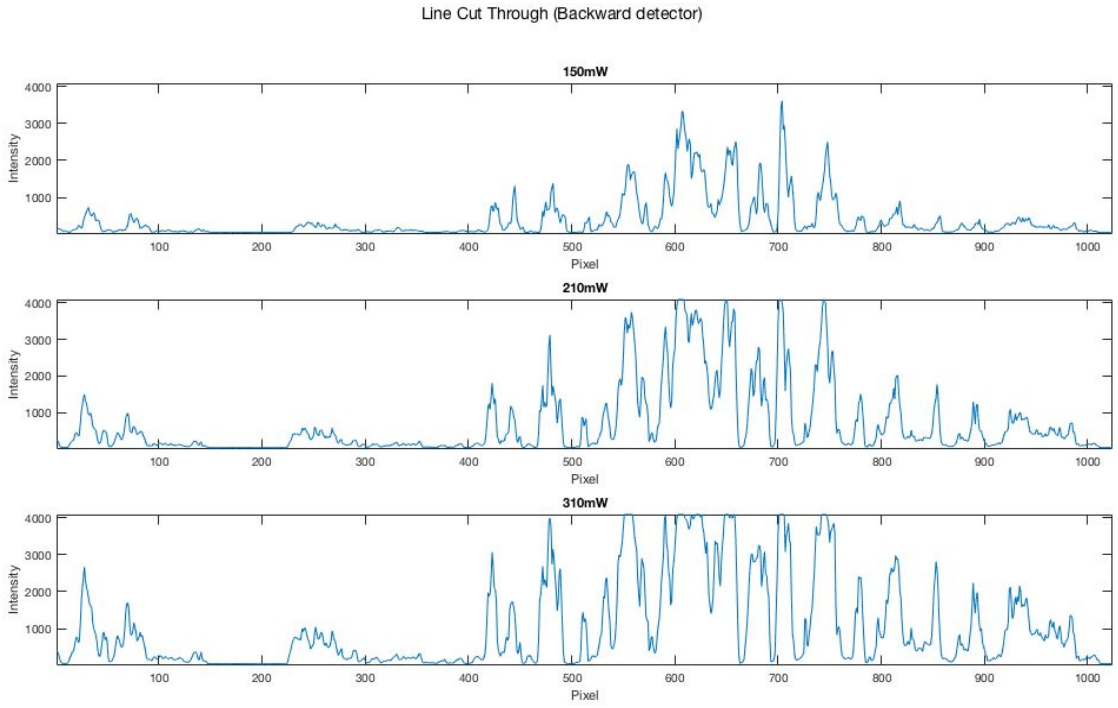

Figure 12. Line cut through averaged over 11 pixels across the center of the backward detector stack at 150, 210 and 310 mW. Areas of high signal (pixels 500-700) are best resolved at low powers before saturation occurs while low signal producing regions (0-100 pixels) are best resolved at high powers.

Our final results for the HDR processing are shown below in figure 13.

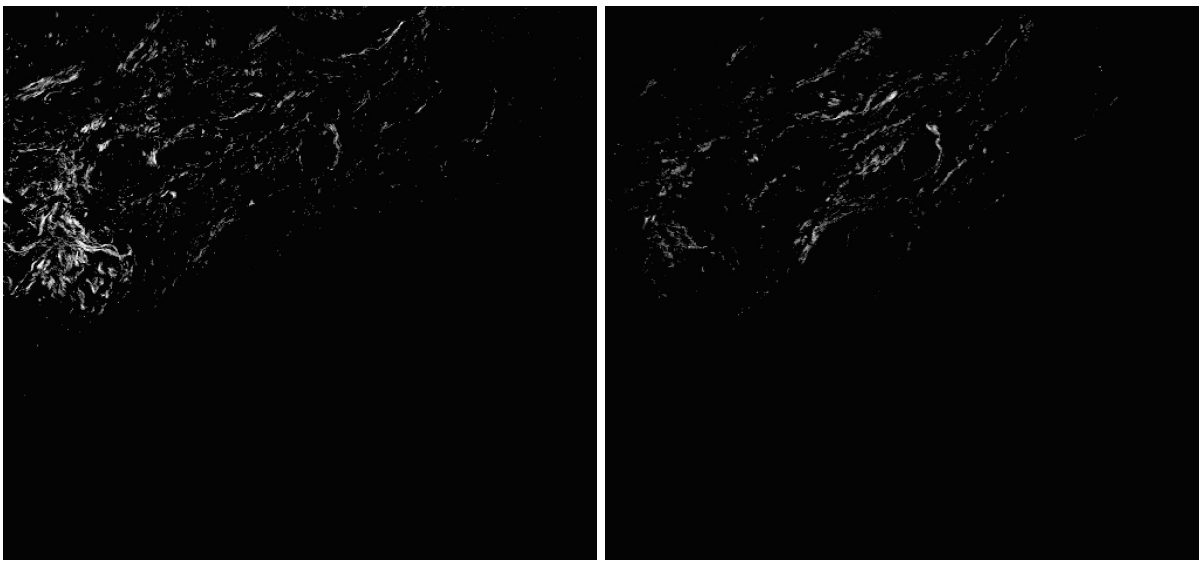

Figure 13. Final HDR results for the forward (right) PMT and backward (left) PMT.

Although these images show the collagen in greater clarity, the HDR processing changes the F/B of the two images (from approximately 6 to 2), making it unreliable for actual diagnosis. We recommend using this processing for making clearer images for demonstration purposes, but not in the actual processing routine.

Track II:

Due to time and lab constraints, the Knox lab testing track is being left as a potential future project.

Hajim School Design Day Demo:

We presented a poster with data from before optimization of the system and after optimization of the system. The data shown included images taken directly from the system and post image processing, as well as plots indicating power and F/B. The poster indicated the process we went through to achieve our final recommendation of 500 mW of power to optimize the system, as well as conclusions and recommendations for our customer in the future.

Conclusions and Recommendations:

After finishing the testing process, we came to several final conclusions. The motivation behind our project was to optimize the SHG scanning system to better predict metastasis in breast cancer tissue through the F/B value. We chose to focus on optimizing the power in order to increase the signal. The initial power input was 100 mW, but after running our experiments and processing the results, we recommend an input power of 500 mW. In order to prevent sample damage, we also advise that the sample not spend more than 5 to 6 minutes in the beam path. It should be noted that these input powers are for the current microscope setup, and correspond to a focal volume power of approximately 80 mW. In a different setup, the input power that matches the recommended focal volume power may be different.

To be more cost effective, we suggest replacing the galvanometer laser scanning system with a less expensive translation stage and replacing the forward detector with a less sensitive PMT to avoid saturation. We also recommend using a less sensitive forward detector than the one that is currently used for both forward and backward to reduce system costs. Finally, we recommend reducing the sensitivity of both PMTs equally by using neutral density filters or a better quality A/D converter in order to prevent saturation.

Future Senior Project:

As there is still much to explore with this project, we recommend that another group work on the SHG microscopy project next year. The group can implement the proposed changes from the track I results on the microscope setup, and carry out the proposed track II research. In this case, we will turn over all of our current data and image processing scripts to help them get started.

References

1. Francesco Banterle, Alessandro Artusi, Kurt Debattista, and Alan Chalmers. Advanced High Dynamic Range Imaging: Theory and Practice . AK Peters (CRC Press), Natick, MA, USA, 2011.
2. K.Burke, M. Smid, R. P. Dawes, M. A. Timmermans, P. Salzman, C. H. M. can Deurzen, David G. Beer, J. A. Foekens, E. Brown. Using Second Harmonic Generation to Predict Patient Outcome in Solid Tumors. 2015, *BMC Cancer 15:929.*
3. Juan M. Bueno, Francisco J. Avila, Pablo Artal, Comparison of Second Harmonic Microscopy images of Collaged-based Ocular Tissues with 800 and 1045 nm. 2017, *Biomedical Optics Vol. 8 No. 11.*
4. *Pantazis, Periklis et al. "Second Harmonic Generating (SHG) Nanoprobes for in Vivo Imaging." Proceedings of the National Academy of Sciences of the United States of America 107.33 (2010): 14535–14540. PMC. Web. 4 Feb. 2018.*
5. Theodossiou T., G. S. Rapti, V. Hovhannisyan, E. Georgiou, K. Politopoulos, D. Yova, Thermally Induced Irreversible Conformational Changes in Collagen Probed by Optical Second Harmonic Generation and Laser-induced Fluorescence. 2002, *Lasers Med Sci 17:34-41.*
6. Williams, Rebecca M., Warren R. Zipfel, Watt W. Webb, 2005, Interpreting Second-Harmonic Generation Images of Collagen I Fibrils. *Biophysical Journal Vol. 88* 1377-1386.
7. Xi. Chen, Oled Nadiarynkh, Sergey Plotnikov, Paul J Campagnola, Second harmonic generation microscopy for quantitative analysis of collagen fibrillar structure. 2012, *Nature America, 10.1038/nprot.2012.009.*